Kafkas Universitesi Veterinar Fakultesi Dergisi
Journal Home-Page: http://vetdergikafkas.org
E-ISSN: 1309-2251

Kafkas Univ Vet Fak Derg
29 (2): 191-199, 2023
DOI: 10.9775/kvfd.2023.29002

RESEARCH ARTICLE

Study on the Skeletal Muscle Transcriptomics of Alxa Gobi Camel and Desert Camel

Tiantian FAN [1,†] Wencheng BAI [1,†] Yuye FU [1] Gan DIG [1] Daleng TAI [2] Sur LIG [3] Tubxin BILIG [4] Demtu ER [1 (*)]

[(†)] *These authors contributed equally to this work*

[1] College of Veterinary Medicine, Inner Mongolia Agricultural University, Key Laboratory of Clinical Diagnosis and Treatment Technology in Animal Disease, Ministry of Agriculture and Rural Affairs, Hohhot, 010018, P.R. CHINA

[2] Animal Disease Prevention and Control Centre of Ejina Banner, Dalaihub Town, Alxa League, Inner Mongolia Autonomous Region, 735400, P.R. CHINA

[3] Comprehensive Support and Technology Promotion Centre of Yingen Sumu, Alxa Left Banner, Alxa League, Inner Mongolia Autonomous Region, 750323, P.R. CHINA

[4] Animal Husbandry and Veterinary Technology Promotion Centre of Alxa League, East Side of Yabrai Road, East City District, Bayanhot Town, Alxa Left Banner, Alxa League, Inner Mongolia Autonomous Region, 750306, P.R. CHINA

ORCIDs: T.T.F. 0000-0002-0005-0126; W.C.B. 0000-0001-7797-8013; Y.Y.F. 0000-0001-5575-5310; G.D. 0000-0003-2165-0005; D.T. 0000-0002-8436-413X; S.L. 0000-0002-3827-8302; T.B. 0000-0003-0269-2250; D.E. 0000-0002-5705-665X

Article ID: KVFD-2023-29002 Received: 05.01.2023 Accepted: 27.03.2023 Published Online: 28.03.2023

Abstract: In order to explore the reasons for the difference in meat production performance between Alxa Gobi camel and Desert camel, we used high-throughput transcriptome sequencing technology, HTSeq, DEGseq and Gene Ontology (GO) and Encyclopedia of Genes and Genomes (KEGG) databases to compare the skeletal muscle gene expression between the two types. A total of 484 classification items were significantly enriched with Gene Ontology (GO) function, among which 246 were related to biological processes, accounting for 50.8%. One hundred eighty-four were related to molecular function, accounting for 38.1%. Fifty-four were related to cell components, accounting for 11.1%. Gene Ontology (GO) function was significantly enriched to 339 up-regulated genes and 108 down-regulated genes. There were 6116 differentially expressed genes annotated in Kyoto Encyclopedia of Genes and Genomes (KEGG) database. Pathway significance enrichment analysis revealed that these genes were involved in 250 biological metabolic pathways, among which 19 had extremely significant differences, 37 were involved in skeletal muscle development, and 13 were involved in fat metabolism. The results showed that Alxa Gobi camel evolved more genes and signaling pathways related to skeletal muscle development and fat deposition than that of Alxa Desert camel during the long evolutionary process, which changed the traits of Alxa Gobi camel and improved its meat performance.

Keywords: *Alxa Bactrian camel, Gene ontology, Kyoto Encyclopedia of genes and genomes, Skeletal muscle transcriptomics*

Alxa Gobi Devesi ve Çöl Devesinin İskelet Kası Transkriptomiği Üzerine Çalışma

Öz: Alxa Gobi devesi ile Çöl devesi arasında et üretim performansındaki farkın nedenlerini araştırmak amacıyla, iki tür arasındaki iskelet kası gen ekspresyonunu karşılaştırmak için yüksek verimli transkriptom dizileme teknolojisi, HTSeq, DEGseq ve Gen Ontolojisi (GO) ve Genler ve Genomlar Ansiklopedisi (KEGG) veri tabanlarını kullandık. Toplam 484 sınıflandırma öğesi, Gen Ontolojisi (GO) işlevi ile önemli ölçüde zenginleştirildi, ki bunların 246'sı biyolojik süreçlerle ilgiliydi ve %50,8'ini oluşturuyordu. Bunların 184'ü moleküler işlevle ilgiliydi ve %38,1'ini oluşturuyordu. Elli dördü ise hücre bileşenleriyle ilgiliydi ve %11,1'ini oluşturuyordu. Gen Ontolojisi (GO) işlevi, 339 upregüle gen ve 108 downregüle gen için önemli ölçüde zenginleştirildi. Kyoto Genler ve Genomlar Ansiklopedisi (KEGG) veri tabanında 6116 farklı eksprese edilmiş gen bulunmaktaydı. Yolak önem zenginleştirme analizi, bu genlerin 250 biyolojik metabolik yolakta yer aldığını, bunlardan 19'unun son derece önemli farklılıklara sahip olduğunu, 37'sinin iskelet kası gelişiminde ve 13'ünün yağ metabolizmasında yer aldığını ortaya koydu. Sonuçlar, Alxa Gobi devesinin uzun evrimsel süreç boyunca Alxa Çöl devesine kıyasla iskelet kası gelişimi ve yağ birikimi ile ilgili daha fazla gen ve sinyal yolu geliştirdiğini, bunun da Alxa Gobi devesinin özelliklerini değiştirdiğini ve et performansını artırdığını göstermiştir.

Anahtar sözcükler: *Alxa Bactrian devesi, Gen ontolojisi, Kyoto Genler ve Genomlar Ansiklopedisi, İskelet kası transkriptomiği*

How to cite this article?

Fan T, Bai W, Fu Y, Gan Dig G, Tai D, Lig S, Bilig T, Er D: Study on the skeletal muscle transcriptomics of Alxa Gobi camel and Desert camel. *Kafkas Univ Vet Fak Derg,* 29 (2): 191-199, 2023.
DOI: 10.9775/kvfd.2023.29002

[(*)] Corresponding author: Demtu ER

Phone: +86-13614713459
E-mail: eedmt@imau.edu.cn

Introduction

The camel belongs to the genus *Camelus* in the *Camelidae* of the order *Artiodactyla* of the *Mammalia* class. The Dromedary camel and the Bactrian camel are divided by the number of humps. Bactrian camels are mainly distributed in Central and Northeast Asia, northern China and Mongolia [1]. China is one of the mainly breeding countries of Bactrian camels, and there are about 411.000 Bactrian camels [2], among which Alxa Bactrian camels are the most numerous and widely distributed, with 220.000 camels, accounting for about half of the whole country. China's Alxa region is the main rearing area for the Alxa Bactrian camels [3]. Alxa Bactrian camel is divided into two types: Gobi camel and Desert camel. Gobi camel is mainly distributed in the Gobi region, while Desert camel is mainly distributed in the desert region [4].

At present, there are many studies focus on their milk, hair and biological characteristics of the Alxa Bactrian camel [4], but there are few reports on its skeletal muscle traits [3-6]. Compared with Desert camels, Gobi camels have higher meat production performance (the net meat weight is 90 kg more than that of Desert camel), smaller diameter and greater density of muscle fiber, and higher content of MyHC I type muscle fiber, while Desert camel muscle fiber has large diameter, small density and high content of MyHC IIb type muscle fiber [4]. Muscle fiber is the basic unit of skeletal muscle and the main component of meat production performance. The development and traits of skeletal muscle fiber determine the meat production performance. Since from the explanation of skeletal muscle traits of double-muscle cattle [7,8] and the application of cloning technology [9,10], genetic modification technology provides a new method for improving meat performance of livestock. In order to further explore the reasons for the differences in meat production performance between Gobi camel and Desert camel, their skeletal muscles were taken as the research objects, and the biceps femoris samples were collected for transcriptome sequencing analysis to obtain gene expression information. We compared and analyzed the biceps femoris samples of Gobi camel and Desert camel in terms of differentially expressed genes, Gene Ontology (GO) function enrichment and Encyclopedia of Genes and Genomes (KEGG) pathway enrichment, in order to reveal the difference of meat production performance between them at molecular level and provide scientific basis for the improvement of meat production performance of Alxa Bactrian camel and the breeding of new strains.

Material and Methods

Ethical Statement

All experimental procedures were approved by the Animal Protection and Use Committee of Inner Mongolia Agricultural University and strictly followed animal welfare and ethical guidelines.

Animal Sample Collection

Five 8-year-old male Alxa Gobi camels and five 8-year-old Desert camels collected 5 g of biceps femoris respectively, washed with alcohol and normal saline once, packed with frozen tubes and marked, temporarily stored in liquid nitrogen, returned to the laboratory and stored in -80ºC refrigerator for a long time. Samples were collected at Western Lifa Slaughterhouse, Alxa League, Inner Mongolia, China.

Extraction of Total RNA and Detection of Total RNA Samples

After the total RNA was extracted from the split liquid of camel biceps femoris by Trizol method (TaKaRa, Kyoto, Japan), the integrity of the total RNA was accurately detected by Agilent 2100 bioanalyzer, the purity of the total RNA (the ratio of OD260/OD280 and OD260/230) was detected by microplate analyzer, and the integrity of the total RNA and the existence of DNA contamination were analyzed by agarose gel electrophoresis (agarose is purchased from Inner Mongolia Chenxin Biology Science and Technology Limited Company, China; markers are purchased from TaKaRa, Kyoto, Japan).

Sample Correlation Analysis

In this study, the square of Pearson correlation coefficient (R^2) was used as an index to judge the similarity of gene expression between samples ($0<R^2<1$, and there is obvious difference when it is higher than 0.8).

Construction, Detection and Computer Sequencing of Library

The sequencing of this experiment was completed by NOVOGENE. The specific situation is shown in *Fig. 1*.

After the construction of the library, the library was initially quantified by using Qubit2.0 Fluorometer, and the library was diluted to 1.5 ng/μL. Then, the insert size of the library was detected by using Agilent 2100 bioanalyzer. After the insert size met expectations, the effective concentration of the library was accurately quantified by qRT-PCR (the effective concentration of the library was higher than 2nM) to ensure the quality of the library.

Data Assembly and Functional Annotation of mRNAs

The original data are stripped of the adapter, which contain N (N means that the base information cannot be determined) and are of low quality (the number of bases with $Q_{phred}<=20$ accounts for more than 50% of the total read length), and filtered to obtain high-quality mRNA clean reads. After analyzing the base mass distribution, CG content and average mass distribution of mRNA clean

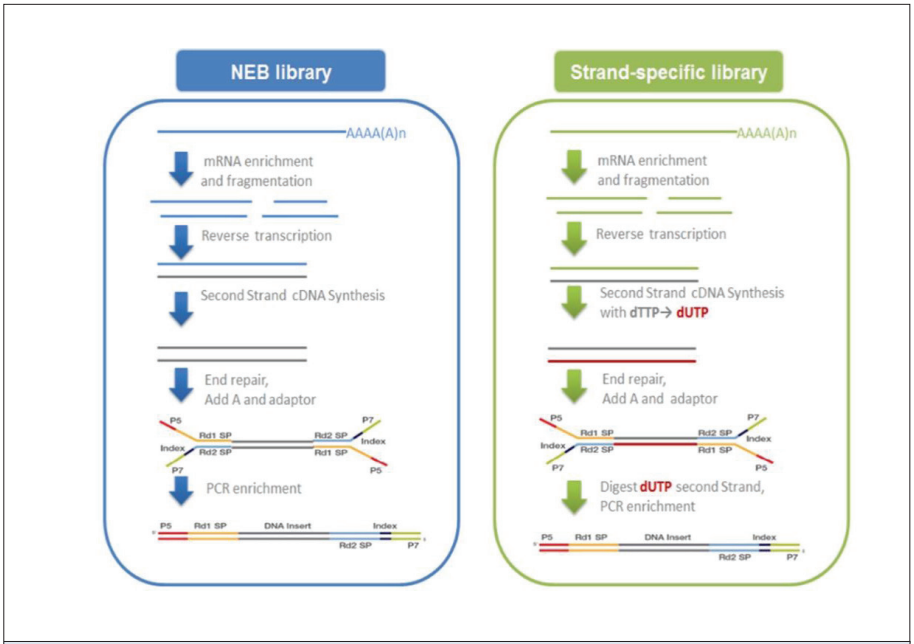

Fig 1. Schematic diagram of library construction

reads, and comparing them with reference genes *(https://www.ncbi.nlm.nih.gov/genome/?term=Camelus+bactrianus)*. HTSeq software was used to study the gene expression level of all the research samples. The selected model was union, and the value of Reads Per Kilo Base of Exon Model Per Million Mapped Reads (FPKM) was determined as 1. Then, the differentially expressed genes were screened by using R language software package DESeq2 (log2(FoldChange)|>0&padj<0.05). Use GOseq software to analyze the GO enrichment of differential genes, calculate the list and number of each term, and calculate the enrichment P-value (hypergeometric distribution, P<0.05 is significant enrichment); In addition, according to KEGG database, the differentially expressed genes were analyzed by KOBAS (2.0) software (hypergeometric distribution, P<0.05 is significant enrichment).

Results

Total RNA Quality Test Results and Integrity Test Electropherogram

The quality test results and integrity test electropherograms of total RNA of 10 samples used in this experiment *(Table 1; Fig. 2)*.

Correlation Between Samples in Quantitative Analysis of Genes

According to the FPKM values calculated for each sample, the correlation coefficients of different samples can

Table 1. *The result of total RNA quality test*

Sample Name	Concentration (ng/μL)	Volume (μL)	Total Quantity(μg)	OD260/280	OD260/230	RIN	Conclusion of Detection
SG_6	43	92	3.956	2	1.33	7.8	A
SG_8	44	92	4.048	1.44	0.9	8	A
SG_10	62	92	5.704	2	1.14	6.6	A
SG_12	35	92	3.22	2.36	0.96	8.4	A
SG_5	192	32	6.144	2	0.76	7.3	A
CG_6	46	92	4.232	1.65	0.94	8.8	A
CG_8	48	92	4.416	2.13	1.39	7.7	A
CG_10	53	92	4.876	1.94	1.55	7.9	A
CG_12	42	92	3.864	1.92	1.09	7.3	A
CG_5	166	32	5.312	2.12	1.09	7	A

SG_6/SG_8/SG_10/SG_12/SG_5 is Alxa Desert camel sample; CG_6/CG_8/CG_10/CG_12/CG_5 is Alxa Gobi camel sample; RIN: RNA integrity number

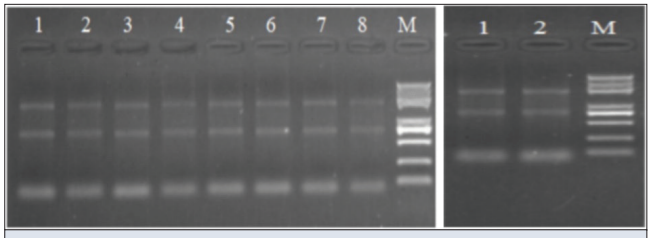

Fig 2. Total RNA extraction electrophoresis results. M: represents Marker (Trans 2K Plus); 1-4 on the left are Alxa Desert camel RNA samples SG_6/SG_8/SG_10/SG_12, 5-8 on the left are Alxa Gobi camel RNA samples CG_6/CG_8/CG_10/CG_12; 1 on the right is Alxa Desert camel SG_5 and 2 on the right is Alxa Gobi camel CG_5

be calculated, so as to obtain the heat map. Analysis of the figure can clarify the differences and repetitions of different samples in each group. If the coefficient is higher, it means that the pattern is closer *(Fig. 3)*.

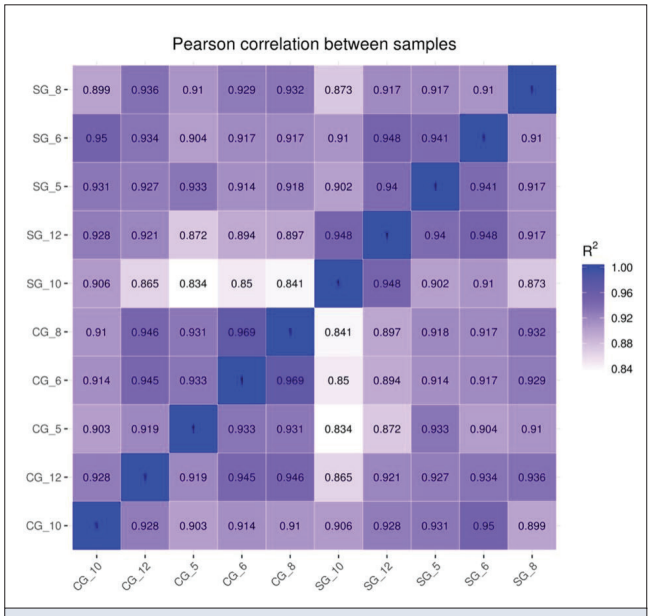

Fig 3. Sample correlation heat map

Gene Expression Distribution in Quantitative Analysis of Genes

Generally, FPKM was selected instead of read count as the expression value of RNA-seq gene. After the FPKM value of all genes is obtained, the gene expression distribution of each sample can be analyzed *(Fig. 4)*.

Differential Gene Statistics in Differential Analysis

The number statistics of differential genes and the criteria for screening differences are shown in *Table 2*.

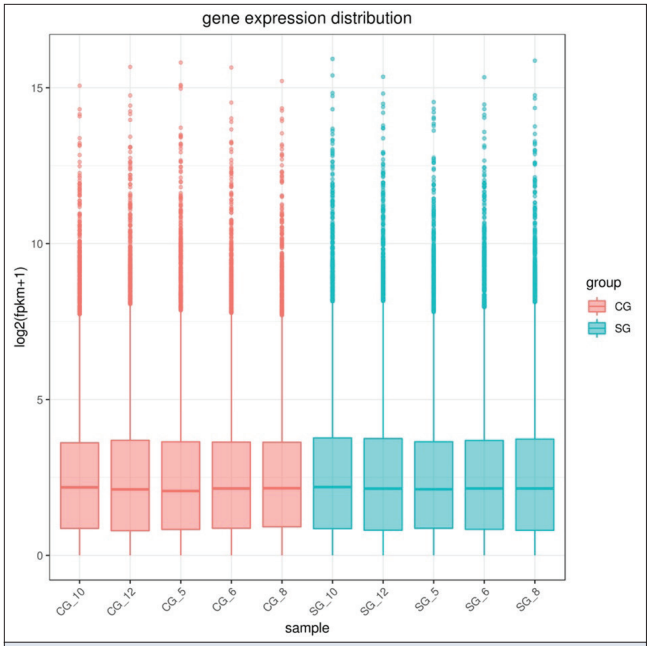

Fig 4. Gene expression level map. The abscissa and ordinate represent the sample name and log2(FPKM+1) respectively. The figure shows a box diagram of each sample, from which the minimum, maximum, median, upper and lower quartile of each sample can be compared and analyzed

The distribution of differentially expressed genes between Alxa Gobi camels (CG) and Alxa Desert camels (SG) is shown in *Fig. 5*.

Venn Diagram of Differential Genes

The sum of all numbers in the Vaine diagram indicated that the total number of differential genes between Alxa Gobi camel and Desert camel was 12592, and the overlap region indicated that the number of common differential genes was 11716, of which 457 genes were unique to Alxa Gobi camel and 419 genes were unique to Alxa Desert camel *(Fig. 6)*.

Differential Gene Clustering

In this experiment, the mainstream hierarchical clustering is used to cluster and analyze the gene expression values, and the genes with similar expression patterns are gathered together to homogenize all the expression data. Genes or samples with similar expression patterns in the heat map are gathered together, and different grid colors indicate the final value after homogenization *(Fig. 7)*.

Table 2. Standard table for number statistics of differential genes and screening differences

Compare	All	Up	Down	Threshold
SG vs CG	489	377	112	DESeq2 padj<0.05 |log2FoldChange|>0.0

Compare: *name of the comparison combination,* ***All:*** *total number of differentially expressed genes in the comparison combination,* ***Up:*** *number of differentially expressed genes up-regulated in the comparison combination,* ***Down:*** *number of differentially expressed genes down-regulated in the comparison combination,* ***Threshold:*** *software and threshold for differential gene screening in the comparison combination. SG is Alxa Desert camel sample; CG is Alxa Gobi camel sample*

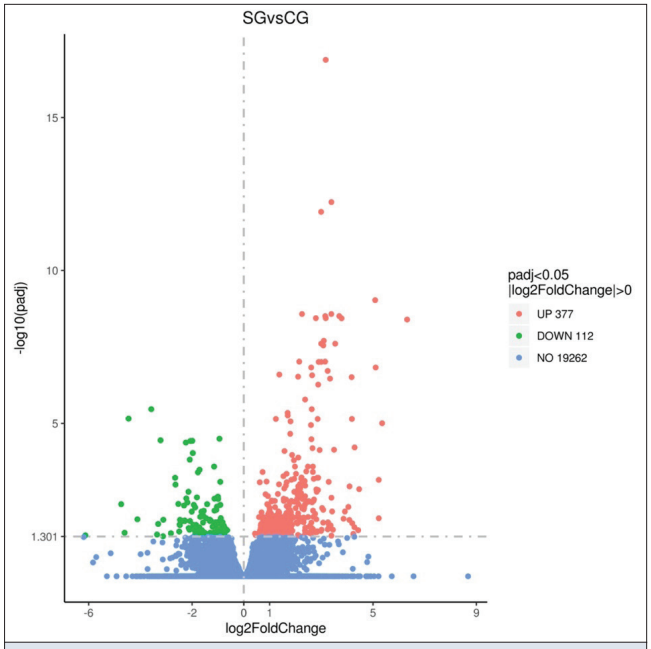

Fig 5. Gene expression level map. The horizontal axis of the figure is the fold change of gene expression (log2FoldChange) between the treatment and control groups, and the vertical axis is the significance level of the difference in gene expression between the treatment and control groups (-log10padj or -log10pvalue). Up-regulated genes are red dots and down-regulated genes are green dots

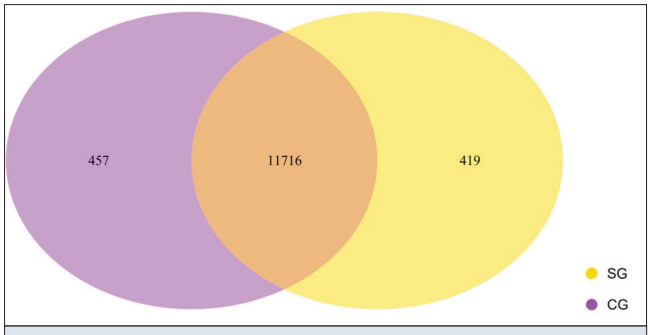

Fig 6. Differential gene Venn map

GO Enrichment Analysis of Differentially Expressed Genes

Among all the genes differentially expressed in the biceps femoris of Alxa Gobi camels and Desert camels, 5695 genes have been annotated, including 148 genes related to biological processes, 66 genes related to cell components and 233 genes related to molecular functions. A total of 484 items were significantly enriched by GO function, among which 246 items were significantly enriched related to biological process, accounting for 50.8%. There were 184 significant enrichment items related to molecular function, accounting for 38.1%. There were 54 significant enrichment items related to cellular component, accounting for 11.1%. The significant enrichment items related to biological process accounted for the largest proportion, but the number of genes involved in biological process was not as large as that involved in molecular function, and

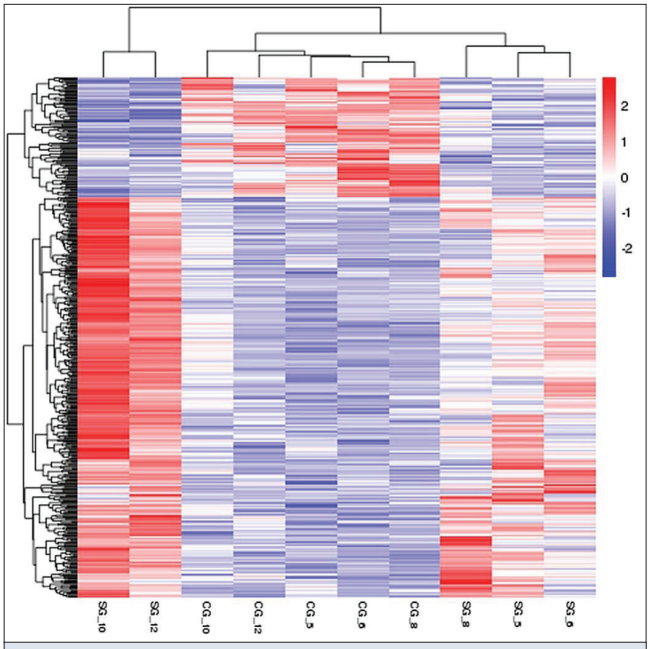

Fig 7. Differential gene cluster map. The colors in the thermogram can only be compared horizontally (the expression of the same gene in different samples), but not vertically (the expression of different genes in the same sample). In horizontal comparison, red indicates high gene expression and blue indicates low gene expression

the genes with extremely significant difference (P<0.01) between Alxa Gobi camel and Desert camel were enriched in molecular function. There were 339 up-regulated genes, including 110 genes related to biological process, 47 genes related to cellular component and 182 genes related to molecular function. A total of 108 genes were down-regulated, among which 38 genes were related to biological process, 19 genes were related to cellular component and 51 genes were related to molecular function.

Analyze the results of GO enrichment analysis, and select the most prominent 30 terms to draw a scatter diagram *(Fig. 8)*.

KEGG Pathway Enrichment Analysis of Differentially Expressed Genes

In this experiment, all differentially expressed genes in biceps femoris of Alxa Gobi camel and Desert camel were enriched by KEGG pathway. The results showed that there were 6116 differentially expressed genes annotated in KEGG database, and the pathway significant enrichment analysis found that these genes participated in 250 biological metabolic pathways, among which 19 pathways were extremely significant differences (P<0.01). There were 37 differential genes involved in skeletal muscle development and 13 differential genes involved in fat metabolism. FoxO signaling pathway, Osteoclast differentiation, and cAMP signaling pathway are involved in skeletal muscle development; in addition, there are two signaling pathways related to lipid metabolism, namely

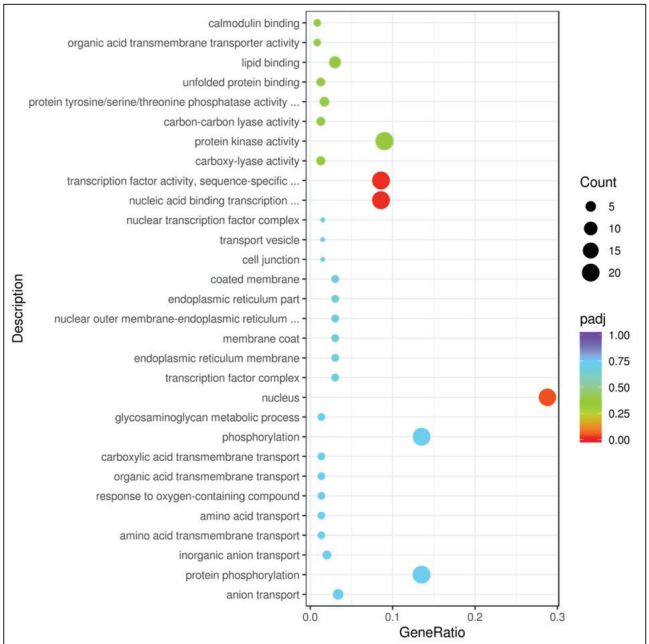

Fig 8. Go enrichment scatter diagram. The ordinate represents Term and the abscissa represents the proportion of the number of differential genes above GO Term in all genes. Each dot represents a specific number of genes, and a different color represents a different significance, ranging from red to purple

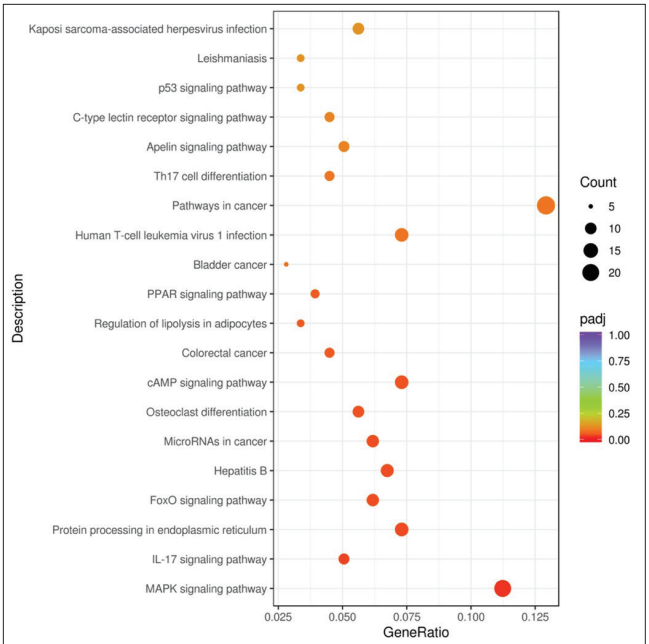

Fig 9. Scatter diagram of KEGG pathway. The abscissa is the ratio of the number of differential genes annotated to the KEGG pathway to the total number of differential genes, the ordinate is the KEGG pathway, the size of the dot represents the number of genes annotated to the KEGG pathway, and the color from red to purple represents the significance of enrichment

Regulation of lipolysis in adipocytes and PPAR signaling pathway.

From the KEGG enrichment results, the most significant 20 KEGG pathways were selected to draw a scatter plot *(Fig. 9)*. Moreover, carefully observing all the signal pathways, MAPK and Pathways in Cancer are rich in the most differentially expressed genes. MAPK and PPAR are rich in up-regulated and down-regulated differentially expressed genes, respectively.

Discussion

In this experiment, the percentage of GC is greater than AT, all of which are over 50%, and the proportion of Q20 of bases in each position is above 97%. Compared with the reference genome, the ratio of the number of reads on the genome is greater than 91.05%, and the number of reads on the gene is greater than 87.75%. At the same time, the FPKM value meets the standard. All these indicate that the sequencing data is reliable and the sequencing quality is high.

In this experiment, the skeletal muscle of Alxa Bactrian camel was analyzed by transcriptome for the first time, and the gene library of Bactrian camel was perfected. A total of 489 differentially expressed genes were screened from the skeletal muscle transcriptome of Alxa Gobi camel and Desert camel, including 377 up-regulated genes and 112 down-regulated genes. Among these genes, candidate genes related to skeletal muscle development and fat deposition were mainly screened.

Among these genes, the genes related to skeletal muscle development are as follows. *FOXO1* gene plays an important role in the transformation of muscle fiber types. *FOXO1* negatively regulates skeletal muscle abundance and is considered to be the key to muscle atrophy [11,12]. *UBE2B* plays an important role in muscle protein homeostasis under catabolism [13]. *EGR1* has been shown to be essential for the expression of key tendon markers and tendine-related *ECM* genes during tendon healing after injury, and *EGR1* controls the balance between bone tissue formation and bone resorption during bone repair [14]. The expression of *SLC25A25* gene is affected by neural pathways, and this gene is a muscle circadian rhythm gene, which is related to muscle thermogenesis and affects the growth and development of skeletal muscle [15]. *ATF4* is a key component of a complex and not fully understood molecular signaling network that leads to muscle atrophy during aging, fasting and imfixation [16]. The normal expression of *AMD1* can improve muscle fibrosis, reduce the overactive pre-fibrotic TGF-b pathway, and lead to improved exercise ability [17]. *ASB5* seems to be essential for muscle recovery after exercise and increases the expression of myogenic hormone, which is a marker of value-added early myogenesis in mammals [18]. *CDKN1A* is involved in the regulation of cell cycle and proliferation of skeletal muscle cells [19,20]. As a muscle-specific regulator,

KLHL30 plays an important role in myoblast proliferation and differentiation [21]. *KLF6* gene can promote the proliferation of skeletal muscle cells, and *miR-148a-3p* can inhibit the proliferation of bovine myoblasts and promote apoptosis through post-transcriptional down-regulation of *KLF6* [22]. *Hspa8* regulates Mef2 protein through chaperonin mediated autophagy to maintain its normal activity, avoid myotonia and mitochondrial function damage, and thus ensure the normal development or regeneration of skeletal muscle [23]. *VGLL2* is a key transcriptional activator of muscle-specific genes, which can be activated by exercise and participate in chronic overload-induced muscle remodeling. It has a great effect on exercise endurance in skeletal muscle, and *VGLL2* is directly or indirectly involved in the specification of mature skeletal muscle fiber characteristics [24-27].

The genes associated with fat deposition are as follows. The *PLIN* gene is involved in lipolysis of neutral lipids and autophagic lipolysis, and regulates lipolysis through the interaction between lipase and lipid droplet protein [28,29]. *LPIN1* plays an important role in adipocyte maturation and adipogenesis [30], and it is essential for de novo synthesis of phospholipids and triglycerides [31].

In terms of signaling pathways, MAPK signaling pathway plays a very important role in adipocyte differentiation [32]. This family controls many important physiological processes, including cell growth, differentiation, proliferation and death, and its pathway is mainly composed of JNK, ERK and p38 pathways [33]. *FOXO1* plays an important role in the regulation of skeletal muscle differentiation and fiber type [34], and is an important transcription factor that determines muscle development and fiber type, but its regulation mode remains controversial. The genes regulated by FoxOs are involved in various pathways, such as metabolic regulation, cell and tissue homeostasis, and immunity [35-38]. Therefore, elucidation of the molecular mechanism of *FOXO1* regulating muscle fiber type and study of FoxO signaling pathway can provide theoretical basis for improving meat quality and new research ideas for genetic improvement and molecular breeding of livestock [39]. The down-regulated genes *PLIN1*, *PLIN4*, *ANGPTL4*, *FABP4* and *PLTP* in the peroxisome proliferator-activated receptor (PPAR) signaling pathway [40] are all genes related to lipid metabolism and lipid deposition.

The results showed that under the influence of living environment and other factors, Alxa Gobi Camel and Desert Camel developed a large number of differential genes in skeletal muscle and fat deposition. These differential genes and their signal pathways changed the phenotypic characteristics of Gobi Camel and improved its meat production performance.

With the development of science and technology, the genetic engineering of livestock [41] is also changing with each passing day. Now, myostatin gene knockout sheep can be efficiently produced by using CRISPR/Cas9 technology and fertilized egg microinjection technology [9]. Compared with the control wild lamb, the weight of these gene knockout sheep is significantly increased. In addition to sheep, livestock genetic engineering has also been used to transform the phenotypic traits of other livestock, such as goats, cattle and pigs [42-45]. Therefore, on the basis of this study, livestock genetic engineering technology can be used to improve the meat production performance of Alashan Bactrian camel and provide scientific basis for cultivating new strains.

Availability of Data and Materials

The datasets during and/or analyzed during the current study available from the corresponding author and can be provided on your request.

Acknowledgements

We thank the Inner Mongolia Science & Technology Plan (No. 201502069) and all partners and laboratory members for their kind help.

Funding Support

The project (No. 201502069) was supported by Inner Mongolia Science & Technology Plan.

Competing Interests

The authors declared that there is no conflict of interest.

Authors' Contributions

TTF and WCB analyzed the experimental results and consulted a large amount of literature to complete the paper writing. YYF and GD conducted a detailed experimental study and summarized the experimental results. DE planned the experimental research program and the implementation process, and guided the writing process of the paper. DT, SL and TB put forward valuable suggestions for the revision and improvement of the paper.

References

1. Zhai B, Niu Q, Liu Z, Yang J, Pan Y, Li Y, Zhao H, Luo J, Yin H: First detection and molecular identification of Borrelia species in Bactrian camel *(Camelus bactrianus)* from Northwest China. *Infect Genet Evol*, 64, 149-155, 2018. DOI: 10.1016/j.meegid.2018.06.028

2. Statistics NBo: China Statistical Yearbook-2021. 2021.

3. Wang F, Bao H, Jiragara B, Yang B, Odongerle, Xu S, Narenbatu, Er D: SNPs AND InDels detection and selection signals identification of alxa bactrian camel by whole-genome resequencing. *J Camel Pract Res*, 27 (1): 69-75, 2020. DOI: 10.5958/2277-8934.2020.00010.7

4. Wenfang, Yuye F, Yang B, Yang H, Borjigin G, Bao H, Narenbatu, Er D: Comparative studies on slaughter performance and skeletal muscle fibre type of alxa gobi camel and desert camel. *J Camel Pract Res*, 26 (1): 63-69, 2019. DOI: 10.5958/2277-8934.2019.00009.2

5. Deng T, Liu T, Tuya, Yang B, Cui A, Surlig, Sharku, Bayartai, Er D: The isolation, culture and identification of skeletal muscle satellite cells from bactrian camel. *J Camel Pract Res*, 26 (3): 219-224, 2019. DOI: 10.5958/2277-8934.2019.00034.1

6. Yang B, Bao H, Wang X, Deng T, Li H, Fu Y, Xu X, Er D: Comparative transcriptome analysis of adipose tissues from bactrian camel. *J Camel Pract Res*, 27 (3): 263-269, 2020. DOI: 10.5958/2277-8934.2020.00035.1

7. McPherron AC, Lee SJ: Double muscling in cattle due to mutations in the myostatin gene. *Proc Natl Acad Sci USA*, 94 (23): 12457-12461, 1997. DOI: 10.1073/pnas.94.23.12457

8. Grobet L, Martin L J, Poncelet D, Pirottin D, Brouwers B, Riquet J, Schoeberlein A, Dunner S, Ménissier F, Massabanda J, Fries R, Hanset R, Georges M: A deletion in the bovine myostatin gene causes the double-muscled phenotype in cattle. *Nat Genet*, 17 (1): 71-74, 1997. DOI: 10.1038/ng0997-71

9. Crispo M, Mulet AP, Tesson L, Barrera N, Cuadro F, dos Santos-Neto PC, Nguyen TH, Creneguy A, Brusselle L, Anegon I, Menchaca A: Efficient generation of myostatin knock-out sheep using CRISPR/Cas9 technology and microinjection into zygotes. *Plos One*, 10 (8):e0136690, 2015. DOI: 10.1371/journal.pone.0136690

10. Dumont NA, Bentzinger CF, Sincennes MC, Rudnicki MA: Satellite cells and skeletal muscle regeneration. *Compr Physiol*, 5 (3): 1027-1059, 2015. DOI: 10.1002/cphy.c140068

11. Russell SJ, Schneider MF: Alternative signaling pathways from IGF1 or insulin to AKT activation and FOXO1 nuclear efflux in adult skeletal muscle fibers. *J Biol Chem*, 295 (45): 15292-15306, 2020. DOI: 10.1074/jbc.RA120.013634

12. Lundell LS, Massart J, Altintas A, Krook A, Zierath JR: Regulation of glucose uptake and inflammation markers by FOXO1 and FOXO3 in skeletal muscle. *Mol Metab*, 20, 79-88, 2019. DOI: 10.1016/j.molmet.2018.09.011

13. Polge C, Leulmi R, Jarzaguet M, Claustre A, Combaret L, Bechet D, Heng AE, Attaix D, Taillandier D: UBE2B is implicated in myofibrillar protein loss in catabolic C2C12 myotubes. *J Cachexia Sarcopeni*, 7 (3): 377-387, 2016. DOI: 10.1002/jcsm.12060

14. Havis E, Duprez D: EGR1 transcription factor is a multifaceted regulator of matrix production in tendons and other connective tissues. *Int J Mol Sci*, 21 (5), 2020. DOI: 10.3390/ijms21051664

15. Nakao R, Shimba S, Oishi K: Ketogenic diet induces expression of the muscle circadian gene Slc25a25 via neural pathway that might be involved in muscle thermogenesis. *Sci Rep*, 7 (1):2885, 2017. DOI: 10.1038/s41598-017-03119-8

16. Adams CM, Ebert SM, Dyle MC: Role of ATF4 in skeletal muscle atrophy. *Curr Opin Clin Nutr Metab Care*, 20 (3): 164-168, 2017. DOI: 10.1097/MCO.0000000000000362

17. Kemaladewi DU, Benjamin JS, Hyatt E, Ivakine EA, Cohn RD: Increased polyamines as protective disease modifiers in congenital muscular dystrophy. *Hum Mol Genet*, 27 (11): 1905-1912, 2018. DOI: 10.1093/hmg/ddy097

18. Liu P, Verhaar AP, Peppelenbosch MP: Signaling size: Ankyrin and SOCS box-containing ASB E3 ligases in action. *Trends Biochem Sci*, 44 (1): 64-74, 2019. DOI: 10.1016/j.tibs.2018.10.003

19. Ren C, Yu M, Zhang Y, Fan M, Chang F, Xing L, Liu Y, Wang Y, Qi X, Liu C, Zhang Y, Cui H, Li K, Gao L, Pan Q, Wang X, Gao Y: Avian leukosis virus subgroup J promotes cell proliferation and cell cycle progression through miR-221 by targeting CDKN1B. *Virology*, 519, 121-130, 2018. DOI: 10.1016/j.virol.2018.04.008

20. Wang J, Song C, Cao X, Li H, Cai H, Ma Y, Huang Y, Lan X, Lei C, Ma Y, Bai Y, Lin F, Chen H: MiR-208b regulates cell cycle and promotes skeletal muscle cell proliferation by targeting CDKN1A. *J Cell Physiol*, 234 (4): 3720-3729, 2019. DOI: 10.1002/jcp.27146

21. Chen G, Yin Y, Lin Z, Wen H, Chen J, Luo W: Transcriptome profile analysis reveals KLHL30 as an essential regulator for myoblast differentiation. *Biochem Biophys Res Commun*, 559: 84-91, 2021. DOI: 10.1016/j.bbrc.2021.04.086

22. Song C, Yang J, Jiang R, Yang Z, Li H, Huang Y, Lan X, Lei C, Ma Y, Qi X, Chen H: miR-148a-3p regulates proliferation and apoptosis of bovine muscle cells by targeting KLF6. *J Cell Physiol*, 234 (9): 15742-15750, 2019. DOI: 10.1002/jcp.28232

23. Wang C, Arrington J, Ratliff AC, Chen J, Horton HE, Nie Y, Yue F, Hrycyna CA, Tao WA, Kuang S: Methyltransferase-like 21c methylates and stabilizes the heat shock protein Hspa8 in type I myofibers in mice. *J Biol Chem*, 294 (37): 13718-13728, 2019. DOI: 10.1074/jbc.RA119.008430

24. Alaggio R, Zhang L, Sung YS, Huang SC, Chen CL, Bisogno G, Zin A, Agaram NP, LaQuaglia MP, Wexler LH, Antonescu CR: A molecular study of pediatric spindle and sclerosing rhabdomyosarcoma: Identification of novel and recurrent VGLL2-related fusions in infantile cases. *Am J Surg Pathol*, 40 (2): 224-235, 2016. DOI: 10.1097/PAS.0000000000000538

25. Agaram NP, LaQuaglia MP, Alaggio R, Zhang L, Fujisawa Y, Ladanyi M, Wexler LH, Antonescu CR: MYOD1-mutant spindle cell and sclerosing rhabdomyosarcoma: An aggressive subtype irrespective of age. A reappraisal for molecular classification and risk stratification. *Mod Pathol*, 32 (1): 27-36, 2019. DOI: 10.1038/s41379-018-0120-9

26. Honda M, Tsuchimochi H, Hitachi K, Ohno S: Transcriptional cofactor Vgll2 is required for functional adaptations of skeletal muscle induced by chronic overload. *J Cell Physiol*, 234(9):15809-15824, 2019. DOI: 10.1002/jcp.28239

27. Honda M, Hidaka K, Fukada SI, Sugawa R, Shirai M, Ikawa M, Morisaki T: Vestigial-like 2 contributes to normal muscle fiber type distribution in mice. *Sci Rep*, 7 (1):7168, 2017. DOI: 10.1038/s41598-017-07149-0

28. Engin A: Fat Cell and Fatty Acid Turnover in Obesity. *Adv Exp Med Biol*, 960, 135-160, 2017. DOI: 10.1007/978-3-319-48382-5_6

29. Cui W, Sathyanarayan A, Lopresti M, Aghajan M, Chen C, Mashek DG: Lipophagy-derived fatty acids undergo extracellular efflux via lysosomal exocytosis. *Autophagy*, 17 (3): 690-705, 2021. DOI: 10.1080/15548627.2020.1728097

30. Zhou F, Fan X, Miao Y: LPIN1 promotes triglycerides synthesis and is transcriptionally regulated by PPARG in buffalo mammary epithelial cells. *Sci Rep*, 12 (1):2390, 2022. DOI: 10.1038/s41598-022-06114-w

31. He J, Zhang F, Tay LWR, Boroda S, Nian W, Levental KR, Levental I, Harris TE, Chang JT, Du G: Lipin-1 regulation of phospholipid synthesis maintains endoplasmic reticulum homeostasis and is critical for triple-negative breast cancer cell survival. *FASEB J*, 31 (7): 2893-2904, 2017. DOI: 10.1096/fj.201601353R

32. Tsai CJ, Nussinov R: Allosteric activation of RAF in the MAPK signaling pathway. *Curr Opin Struct Biol*, 53, 100-106, 2018. DOI: 10.1016/j.sbi.2018.07.007

33. Asl ER, Amini M, Najafi S, Mansoori B, Mokhtarzadeh A, Mohammadi A, Lotfinejad P, Bagheri M, Shirjang S, Lotfi Z, Rasmi Y, Baradaran B: Interplay between MAPK/ERK signaling pathway and MicroRNAs: A crucial mechanism regulating cancer cell metabolism and tumor progression. *Life Sci*, 278:119499, 2021. DOI: 10.1016/j.lfs.2021.119499

34. Marie K, Daniel P, Anne G-B, Carole C, François LL, Carla F, Veronique M, Nadege C, Marie-Pierre C, Adeline D-G, Jean-Yves B, Franck T: SRF-FOXO1 and SRF-NCOA1 fusion genes delineate a distinctive subset of well-differentiated rhabdomyosarcoma. *Am J Surg Pathol*, 44 (5): 607-616, 2020. DOI: 10.1097/PAS.0000000000001464

35. Liu L, Cheng Z: Forkhead box O (FoxO) Transcription factors in autophagy, metabolic health, and tissue homeostasis. **In**, Turksen K (Ed): Autophagy in Health and Disease. Stem Cell Biology and Regenerative Medicine. Humana Press, Cham. DOI: 10.1007/978-3-319-98146-8_4

36. Cheng Z: The FoxO-autophagy axis in health and disease. *Trends Endocrinol Metab*, 30 (9): 658-671, 2019. DOI: 10.1016/j.tem.2019.07.009

37. Martins R, Lithgow GJ, Link W: Long live FOXO: unraveling the role of FOXO proteins in aging and longevity. *Aging Cell*, 15 (2): 196-207, 2016. DOI: 10.1111/acel.12427

38. Calissi G, Lam EW, Link W: Therapeutic strategies targeting FOXO transcription factors. *Nat Rev Drug Discov*, 20 (1): 21-38, 2021. DOI: 10.1038/s41573-020-0088-2

39. Yadav H, Devalaraja S, Chung ST, Rane SG: TGF-beta1/Smad3 pathway targets PP2A-AMPK-FoxO1 signaling to regulate hepatic gluconeogenesis. *J Biol Chem*, 292 (8): 3420-3432, 2017. DOI: 10.1074/jbc.M116.764910

40. Christofides A, Konstantinidou E, Jani C, Boussiotis VA: The role of peroxisome proliferator-activated receptors (PPAR) in immune responses. *Metabolism*, 114:154338, 2021. DOI: 10.1016/j.metabol.2020.154338

41. Van Eenennaam AL, De Figueiredo Silva F, Trott JF, Zilberman D: Genetic engineering of livestock: The opportunity cost of regulatory delay. *Annu Rev Anim Biosci*, 9, 453-478, 2021. DOI: 10.1146/annurev-

animal-061220-023052

42. Proudfoot C, Carlson DF, Huddart R, Long CR, Pryor JH, King TJ, Lillico SG, Mileham AJ, McLaren DG, Whitelaw CB, Fahrenkrug SC: Genome edited sheep and cattle. *Transgenic Res*, 24 (1): 147-153, 2015. DOI: 10.1007/s11248-014-9832-x

43. Qian L, Tang M, Yang J, Wang Q, Cai C, Jiang S, Li H, Jiang K, Gao P, Ma D, Chen Y, An X, Li K, Cui W: Targeted mutations in myostatin by zinc-finger nucleases result in double-muscled phenotype in Meishan pigs. *Sci Rep*, 5:14435, 2015. DOI: 10.1038/srep14435

44. Wang X, Niu Y, Zhou J, Yu H, Kou Q, Lei A, Zhao X, Yan H, Cai B, Shen Q, Zhou S, Zhu H, Zhou G, Niu W, Hua J, Jiang Y, Huang X, Ma B, Chen Y: Multiplex gene editing via CRISPR/Cas9 exhibits desirable muscle hypertrophy without detectable off-target effects in sheep. *Sci Rep*, 6:32271, 2016. DOI: 10.1038/srep32271

45. Wang X, Niu Y, Zhou J, Zhu H, Ma B, Yu H, Yan H, Hua J, Huang X, Qu L, Chen Y: CRISPR/Cas9-mediated MSTN disruption and heritable mutagenesis in goats causes increased body mass. *Anim Genet*, 49 (1): 43-51, 2018. DOI: 10.1111/age.12626